

12 AUG 1948

# NATIONAL ADVISORY COMMITTEE FOR AERONAUTICS

TECHNICAL NOTE

No. 1674

ESTIMATION OF EFFECTIVENESS OF FLAP-TYPE  
CONTROLS ON SWEPTBACK WINGS

By John G. Lowry and Leslie E. Schneiter

Langley Aeronautical Laboratory  
Langley Field, Va.



QCE  
142

Washington  
August 1948

**FOR REFERENCE**

NOT TO BE TAKEN FROM THIS ROOM

**NACA LIBRARY**

LANGLEY MEMORIAL AERONAUTICAL  
LABORATORY  
Langley Field, Va.

## NATIONAL ADVISORY COMMITTEE FOR AERONAUTICS

TECHNICAL NOTE NO. 1674

## ESTIMATION OF EFFECTIVENESS OF FLAP-TYPE

## CONTROLS ON SWEEPBACK WINGS

By John G. Lowry and Leslie E. Schreiber

## SUMMARY

An analysis has been made of the low-speed lift, rolling, and pitching characteristics of flap-type controls on a series of swept-back wings, and methods are presented for estimating these characteristics.

The methods developed are essentially modifications of the existing methods used in estimating the effectiveness of flap-type controls on unswept wings. Satisfactory results may be obtained by each method for flap-type controls on swept wings having from  $0^\circ$  to  $60^\circ$  sweep, aspect ratios from 2.50 to 6.00, and taper ratios between 0.4 and 1.0. The control parameters apply only in the range where the variations with angle of attack and flap deflection are linear.

## INTRODUCTION

In an attempt to extend the maximum speed of airplanes into the transonic and supersonic speed range, an ever increasing number of airplanes are being designed with swept wings. The use of these plan forms has introduced the need for control-surface data on swept wings similar to those already in existence for unswept wings (references 1 to 8), which allow for the prediction of control-surface characteristics within small limits.

At the present time information on the behavior of controls in the transonic speed range is too meager to permit the development of a rational design procedure that applies at transonic speeds; hence, the design of control surfaces for transonic airplanes must still be based primarily on low-speed considerations.

A summary of the results of several low-speed wind-tunnel investigations of control effectiveness on sweptback wings (data obtained in the Langley 300 MPH 7- by 10-foot tunnel) and a discussion of the development of two methods of estimating the effectiveness characteristics of flap-type controls on sweptback wings are presented herein.

## SYMBOLS

For the purposes of this paper, the chords and spans of the swept wings are measured parallel and perpendicular to the plane of symmetry, and the sweep angle is that of the wing leading edge (fig. 1). The control-surface deflections are measured in a plane perpendicular to the control hinge line. The term flap is used herein to designate any type of control surface, regardless of its application. The "unswept" wing panel represents a wing that would be obtained if the swept wing were rotated about the midpoint of the root chord until the 50-percent-chord line is perpendicular to the plane of symmetry. The tip is cut off parallel to the plane of symmetry. The chords in this case are measured perpendicular to the 50-percent-chord line. All primed values refer to the "unswept" wing.

$C_L$	wing lift coefficient ( $L/qS$ where $L$ is lift of complete wing or twice lift of semispan wing)
$c_l$	section lift coefficient
$C_m$	wing pitching-moment coefficient ( $M/qS\bar{c}$ where $M$ is pitching moment of complete wing or twice pitching moment of semi-span wing)
$c_m$	section pitching-moment coefficient
$C_l$	rolling-moment coefficient ( $L/qSb$ where $L$ is rolling moment produced by deflection of one aileron on a complete wing)
$S$	area of complete wing
$b$	span of complete wing, measured on a line perpendicular to model plane of symmetry
$b_f$	span of flap, measured on a line perpendicular to wing plane of symmetry
$\bar{c}$	wing mean aerodynamic chord $\left( \frac{2}{S} \int_0^{b/2} c^2 dy \right)$
$c$	wing local chord, measured in planes parallel to model plane of symmetry
$c_f$	chord of flap, measured in planes parallel to wing plane of symmetry
$c_s$	wing root chord

$\lambda$	wing taper ratio (Wing tip chord/Wing root chord)
$y$	lateral distance from plane of symmetry
$y_1$	lateral distance from plane of symmetry to inboard end of flap
$y_0$	lateral distance from plane of symmetry to outboard end of flap
$d$	distance from center of pressure of incremental lift load to moment axis, measured in planes parallel to wing plane of symmetry
$A$	aspect ratio ( $b^2/S$ )
$q$	free-stream dynamic pressure ( $\frac{1}{2}\rho V^2$ )
$\rho$	mass density of air
$V$	free-stream air velocity
$\alpha$	wing angle of attack, measured in model plane of symmetry
$\delta$	control-surface deflection, measured in a plane perpendicular to control-surface hinge line, positive when control-surface trailing edge is below wing chord plane
$\Lambda$	wing sweep angle, that is, angle between wing leading edge and a perpendicular to wing plane of symmetry
$\alpha_\delta$	flap effectiveness parameter, that is, effective change in wing angle of attack caused by unit angular change in control-surface deflection
$C_l/\Delta\alpha$	rolling-moment coefficient caused by a unit difference in wing angle of attack of various right and left parts of a complete wing
$K_1$	aspect-ratio correction factor for $C_l/\Delta\alpha$
$K_2$	taper-ratio correction factor for $C_l/\Delta\alpha$
$K_3$	aspect-ratio correction factor for $C_{l\delta}/\alpha_\delta$
$M$	Mach number ( $V/a$ )
$a$	speed of sound
$R$	Reynolds number ( $\rho V \bar{c}/\mu$ )

$\mu$  coefficient of viscosity of air

$$C_{L\delta} = \left( \frac{\partial C_L}{\partial \delta} \right)_{\alpha}$$

$$C_{l\delta} = \left( \frac{\partial C_l}{\partial \delta} \right)_{\alpha}$$

$$C_{m\delta} = \left( \frac{\partial C_m}{\partial \delta} \right)_{\alpha}$$

The subscript  $\alpha$  indicates the factor held constant. All slopes were measured or calculated in the range of  $\alpha = 0^\circ$  and  $\delta = 0^\circ$ .

The rolling effectiveness parameter presented herein represents the aerodynamic effects on a complete wing produced by the deflection of the aileron on only one semispan of the complete wing. The lift and pitching effectiveness parameters represent the aerodynamic effects of deflection in the same direction of the flaps on both semispans of the complete wing.

#### EXPERIMENTAL DATA

In order to determine to what extent the design procedure for controls on unswept wings would have to be modified for swept wings, a semispan-wing model was tested essentially unswept ( $\Lambda = 6.3^\circ$ ) and at sweep angles of  $30^\circ$ ,  $40^\circ$ , and  $51.3^\circ$ . (See models 1 to 4, table I.) The aspect ratio of the wings varied from 6.23 for the  $6.3^\circ$  swept wing to 3.43 for the  $51.3^\circ$  swept wing. The wing was equipped with a variable-span plain-sealed flap having a chord 20 percent of the chord of the "unswept" wing. The tests were performed in the Langley 300 MPH 7- by 10-foot-tunnel at a Mach number of about 0.12 and at Reynolds numbers of about  $1.55 \times 10^6$  for the  $6.3^\circ$  swept wing and  $2.2 \times 10^6$  for the  $51.3^\circ$  swept wing.

The variation of the rate of change of rolling-moment coefficient with deflection  $C_{l\delta}$  with span of aileron for the various angles of sweep, as obtained for models 1 to 4, is shown in figure 2. The aileron for these investigations extended inboard from the tip. The variation

of  $C_{l\delta}$  with sweep shown here also includes the effect of aspect ratio which varied from 6.23 for the  $6.3^\circ$  swept wing to 3.43 for the  $51.3^\circ$  swept wing. As the sweep is increased and as the aspect ratio decreases, the values of  $C_{l\delta}$  decrease appreciably. In addition, the percent decrease in the value of  $C_{l\delta}$  with increasing sweep is greater for short-span tip ailerons than for ailerons of approximately 0.50 semispan or greater.

The lift effectiveness parameter  $C_{L\delta}$  obtained from these same models showed about the same variation with sweep as did the rolling-moment effectiveness parameter; that is, there was a decrease in  $C_{L\delta}$  with increase in sweep and with decrease in aspect ratio. (See fig. 3.) The pitching-moment effectiveness parameter  $C_{m\delta}$  showed about the same variation with sweep as did the rolling-moment effectiveness parameter except for the  $6.3^\circ$  swept wing (fig. 4). The linear variation of  $C_{m\delta}$  with flap span on the  $6.3^\circ$  swept wing (fig. 4) and the drop-off of effectiveness of the short-span tip flaps is the type of variation that would be predicted from the theoretical treatment presented in reference 8. The pitching moment produced by a given increment of flap span is proportional to the product of the incremental lift produced by the flap and the chordwise distance from the center of pressure of the incremental load to the axis about which the moments are taken (the wing aerodynamic center for these tests). The decreasing pitch effectiveness of a given increment of span of flap for sweep angles greater than  $30^\circ$  indicates that the incremental-lift-producing effectiveness of the flap decreases faster than the moment arm of this incremental lift increases.

## METHODS

The results of an analysis of the aforementioned wind-tunnel data led to the development of two methods of estimating the lift and rolling effectiveness parameters  $C_{L\delta}$  and  $C_{l\delta}$ , respectively, and one method of estimating the pitching effectiveness parameter  $C_{m\delta}$ .

### Method I

Rolling effectiveness parameter  $C_{l\delta}$ .— In order to make figure 2 of a more general nature, the data were reduced to a form similar to that presented in reference 2 — that is,  $C_l/\Delta\alpha$ , the rolling-moment coefficient caused by a unit difference in wing angle of attack of various right and left parts of a complete wing. Simple sweep theory indicates that only the component of the free-stream dynamic pressure  $q$  in the direction perpendicular to the wing leading edge has a bearing on the effectiveness of a flap; hence, the effective value of  $q$  at

constant free-stream velocity varies as  $\cos^2\Lambda$ . On this basis, the values of  $C_{l\delta}$  (fig. 2) at each spanwise station were divided by  $\cos^2\Lambda$  and the value of the flap effectiveness parameter  $\alpha_\delta$  ( $\Delta\alpha/\Delta\delta$  from reference 3) for the flap on the "unswept"-wing panel. No aspect-ratio or taper-ratio corrections were applied since the "unswept"-wing values of these factors for each of the swept wings are sufficiently near the aspect-ratio and taper-ratio values of the  $6.3^\circ$  swept wing to make corrections unnecessary. This reduction brought the curves into approximate agreement except for the short-span tip ailerons on the  $40^\circ$  and  $51.3^\circ$  swept wings. A curve of the average of the values computed from the curves of figure 2 and from the theoretical values of reference 2 for a comparable aspect ratio and taper ratio is presented in figure 5.

In order to use this chart for design purposes, the values must be corrected for aspect ratio, taper ratio, and flap chord. The rolling effectiveness parameter  $C_{l\delta}$  may be calculated from the formula

$$C_{l\delta} = \left(\frac{C_l}{\Delta\alpha}\right)_u K_1 K_2 \alpha_\delta \cos^2\Lambda$$

The value of  $(C_l/\Delta\alpha)_u$  can be obtained from the appropriate curve in figure 5 (the subscript  $u$  indicates the value of  $C_l/\Delta\alpha$  for a wing of aspect ratio 6.00 and taper ratio 0.5); the aspect-ratio correction factor  $K_1$  can be obtained from figure 6 and is the ratio of  $C_l/\Delta\alpha$  for the aspect ratio of the "unswept" wing to the value of  $C_l/\Delta\alpha$  for aspect ratio 6.00, both values being obtained from reference 2 for taper ratio 0.5; the taper-ratio correction factor  $K_2$  can be obtained from figure 6 and is the ratio of the value of  $C_l/\Delta\alpha$  for taper ratio of the "unswept" wing to the value of  $C_l/\Delta\alpha$  for taper ratio 0.5, both values again being obtained from reference 2 for aspect ratio 6.00; the flap effectiveness parameter  $\alpha_\delta$  is given in figure 7 and is based on the "unswept" flap chord ratio; and  $\Lambda$  is the sweep of the wing leading edge.

For sweep angles from  $0^\circ$  to  $30^\circ$ , values of  $C_l/\Delta\alpha$  should be picked from the averaged curve in figure 5. Values for wings of higher sweeps may be obtained by interpolation between the averaged curve and the curve for the  $51.3^\circ$  swept wing. In order to calculate the rolling effectiveness of ailerons having chord ratios  $c_f^*/c^*$  which vary across the aileron span, the value of  $\alpha_\delta$  for the value of  $c_f^*/c^*$  at the inboard end of the aileron should be used.

The data of figure 2 and, hence, the curves of  $C_l/\Delta\alpha$  of figure 5 apply to ailerons at spanwise locations other than those starting at the tip. The value of  $C_l/\Delta\alpha$  for an element of aileron covering any spanwise part of the wing is the difference between  $C_l/\Delta\alpha$  at the inboard end of the aileron and  $C_l/\Delta\alpha$  at the outboard end of the aileron.

Lift effectiveness parameter  $C_{L\delta}$ .— The lift data presented in figure 3 were reduced to the parameter  $C_{L\delta}/\alpha_\delta$  by the same method used to reduce the roll data; that is, the value of  $C_{L\delta}$  at each spanwise station was divided by  $\cos^2\Lambda$  and  $\alpha_\delta$  of the "unswept" control. This reduction brought all the data into general agreement except for the small span controls on the  $51.3^\circ$  swept wing which again showed a loss in lifting effectiveness. An averaged curve of  $C_{L\delta}/\alpha_\delta$  is presented in figure 8. The values of  $C_{L\delta}$  may be computed for wings of other sweep angles, aspect ratios, and flap spans by the formula

$$C_{L\delta} = \left( \frac{C_{L\delta}}{\alpha_\delta} \right)_u \alpha_\delta K_3 \cos^2\Lambda$$

The value of  $\left( \frac{C_{L\delta}}{\alpha_\delta} \right)_u$  is obtained from figure 8 (the subscript  $u$  indicates the value of  $C_{L\delta}/\alpha_\delta$  for a wing of aspect ratio 6.00 and taper ratio 0.5); the flap effectiveness parameter  $\alpha_\delta$  is obtained from figure 7; and the aspect-ratio correction factor  $K_3$  is obtained from figure 9. The aspect-ratio correction factor  $K_3$  is the ratio of the slope of the lift curve  $C_{L\alpha}$  of the "unswept" wing to the slope of the lift curve for a wing of aspect ratio 6.00. The data used in calculating this curve were obtained from complete models and isolated wings in the Langley 7- by 10-foot tunnel. No taper-ratio correction appears to be necessary, at least not for taper ratios of 0.4 to 1.0.

Lift data on unswept wings indicate that the lift effectiveness of flaps is different for flaps starting at the wing root and for those starting at the wing tip. Hence, it appears that this method must be limited to the prediction of the characteristics of flaps starting at the wing tip only.

#### Method III

Pitching effectiveness parameter  $C_{m\delta}$ .— Any attempts to correlate the pitching-moment data of figure 4 by methods similar to method I were unsuccessful. A method for calculating the pitching effectiveness



of partial span flaps is presented in reference 8. This method is based on calculation of the theoretical spanwise load distribution by the method of reference 1 and the chordwise location of the center of pressure of each spanwise increment of this load. The pitching moment about the wing aerodynamic center produced by this incremental load may then be calculated at several spanwise stations and the resulting curve should be integrated to determine the total pitching-moment effectiveness of the flap. The method of reference 8 does not, however, take into consideration any effects of sweep on the magnitude or distribution of the spanwise loading.

On the basis of the results of the calculations of method I, it appeared that unless sweep corrections were applied erroneous results would be obtained if the method of reference 8 was used directly to calculate the pitching effectiveness of flaps on highly swept wings. The method presented in reference 8 was therefore revised to incorporate such sweep corrections and is re-presented herein with the appropriate sweep corrections applied.

The incremental lift caused by flap deflection at a constant angle of attack was obtained by the influence-lines method of reference 1. Inasmuch as the data of reference 1 apply rigorously only to wing shapes shown in that report, a chord correction was necessary.

The spanwise loading factor  $\frac{c_l(c/c_s)}{\alpha}$  at each spanwise station for the wing in reference 1 most similar to the swept wing under consideration with regard to taper ratio was multiplied by the ratio of the chord of a wing having a straight leading and trailing edge, a square tip, and a taper ratio the same as that of the wing in reference 1 to the chord of the wing in reference 1. The two wings were compared in such a manner that this ratio was 1.0 at the wing root.

The spanwise loading factors of reference 1 are presented for several aspect ratios and taper ratios. The distribution of  $\frac{c_l(c/c_s)}{\alpha}$  for the flap span under consideration, corrected for chord as previously noted, was determined for each of the aspect ratios in reference 1 at the taper ratio most nearly corresponding to the taper ratio of the swept wing under consideration. The spanwise-load-distribution factors presented in figure 2 of reference 1 are those produced by a flap deflected on only one-half of a complete wing. In order to determine the total spanwise loading on one-half of a complete wing caused by deflection of a flap on both halves of the wing, the loading at a negative (left) wing station must be added to the loading at the same station on the positive (right) wing.

The values of the spanwise loading factor at each spanwise station are then determined by extrapolation or interpolation of these data to the aspect ratio of the "unswept" wing corresponding to the swept wing under consideration.

The data of reference 1 give the value of incremental lift produced by flaps that create an effective change in angle of attack of 1 radian over the flapped part of the wing. It is assumed that the incremental lift produced by the flap is directly proportional to the effective angle of attack produced by the flap. Thus, in order to convert such data to the incremental lift produced by a different flap deflection, it is necessary to determine the incremental angle of attack produced by that flap deflection. As has been previously mentioned, the incremental angle of attack produced by flap deflection is indicated by the flap effectiveness parameter  $\alpha_6$  as shown in figure 7 for various percent-chord flaps. The incremental section lift coefficient  $\Delta c_l$  at each spanwise station produced by unit flap deflection may now be calculated by the following formula:

$$\Delta c_l = \frac{c_l(c/c_B)}{\alpha} \frac{\alpha_6}{57.3} \frac{c_B}{c} \cos^2 A \quad (1)$$

where  $\frac{c_l(c/c_B)}{\alpha}$  is the spanwise loading factor previously calculated from reference 1,  $\alpha_6$  is the flap effectiveness parameter (taken from fig. 7) of the flap having the chord ratio  $c_F/c$ ,  $c_B/c$  is the chord ratio of the wing in question, and  $A$  is the sweep angle of the wing leading edge.

The pitching-moment effectiveness parameter  $C_{m6}$  may be calculated by multiplying the incremental lift load at each spanwise station as computed by formula (1) by the corresponding moment arm - that is, the distance between the local center of pressure of the incremental lift load and the moment axis. Mechanical integration of the spanwise distributions of pitching moments thus obtained yields the total pitching effectiveness of the flap  $C_{m6}$ . The chordwise variation of the local center of pressure of the incremental lift load across the span of the wing was determined by a method, the reasoning behind which is discussed in detail in reference 8. Briefly, the method involves placing the line of centers of pressure of the incremental lift loads over the flapped part of the wing along the percent chord line (in the stream direction) indicated by the center-of-pressure data shown in figure 10. (The data in this figure were determined from the data of references 8 to 11.) The line of centers of pressure of the incremental lift loads over the unflapped part of the wing are laid out on a faired line which intersects the line of centers of pressure over the flapped part of the wing at the inboard end of the flap and become tangent to the wing quarter-chord line at a point approximately 30 percent of the wing semispan inboard of the inboard end of the flap, as shown in figure 11.

Lift effectiveness parameter  $C_{L\delta}$ .— The lift effectiveness parameter  $C_{L\delta}$  may be calculated as an incidental to the calculation of  $C_{m\delta}$  by mechanically integrating the area under the curve of  $\Delta c_l$  (determined by formula (1)) against spanwise location.

Rolling effectiveness parameter  $C_{l\delta}$ .— The rolling effectiveness parameter  $C_{l\delta}$  may also be computed. The same spanwise lift distribution used to determine  $C_{L\delta}$  may be mechanically integrated to determine the moment of the load about the wing center line. The rolling-moment coefficients so computed are somewhat in error since they include the carry-over effects of a flap deflected in the same direction on the remaining half of the complete wing. The rolling-moment coefficients so computed may be readily corrected for the carry-over effects by the method of figure 13 of reference 12. For illustrative purposes, a sketch of the incremental section lift and pitching-moment coefficients produced by a partial-span flap on a swept wing is shown in figure 11.

#### ACCURACY OF METHOD

In order to determine the reliability of the two methods of predicting the various control parameters on wings having various geometric characteristics, values of  $C_{L\delta}$  and  $C_{l\delta}$  were estimated by method I and values of  $C_{L\delta}$ ,  $C_{l\delta}$ , and  $C_{m\delta}$  were estimated by method II for the wings shown in table I. These estimated values are compared with the experimentally determined values.

Comparisons of estimated  $C_{L\delta}$  with experimental  $C_{L\delta}$  and estimated  $C_{l\delta}$  with experimental  $C_{l\delta}$  are presented in figures 12 and 13, respectively, for method I and in figures 14 and 15, respectively, for method II. It appears from the scatter of points around the line of agreement that both methods give equally good agreement in calculating  $C_{L\delta}$ . For calculating  $C_{l\delta}$ , method I appears to give somewhat better agreement with the experimental results than does method II. In general, method II underestimates the rolling effectiveness. The spanwise-load-distribution factors presented in reference 1 are for wings with round tips, whereas all the experimental data used in the comparison are for wings having essentially square tips. The difference between the load on a wing with a round tip and the load on a wing with a square tip would be small in regard to lift or pitching moment. However, the load difference between the two wing shapes would be located near the wing tip and would consequently be expected to have some effect upon the rolling moments.

With the exception of the estimated values for models 2 and 15 (table I), the agreement of estimated  $C_{m\delta}$  with the experimental results was excellent, as is shown in figure 16.

It was noted in the correlation for method I that the lift and rolling effectiveness data for model 2 failed to correlate with the comparable data for models 1, 3, and 4, the results for model 2 being, in general, too high. The comparisons of calculated with experimental lift and rolling effectiveness shown in figures 14 and 15 for method II seem to substantiate the belief that the data for model 2 are in error. Since the lift, rolling, and pitching effectiveness of a given flap are so closely interrelated, it may also be assumed that the pitching effectiveness data of model 2 are also somewhat in error and hence would fail to correlate with the data of other models.

In general, it may be stated that both methods of calculating the control effectiveness parameters gave satisfactory results for sweptback wings having sweep angles from  $0^\circ$  to  $60^\circ$ , aspect ratios from 2.50 to 6.00, taper ratios from 0.4 to 1.0 and having conventional low drag or circular-arc airfoils. Both of these methods are, of course, limited to the range wherein lift has a linear variation with both wing angle of attack and flap deflection. As was previously mentioned, lift data on unswept wings indicate that the lift effectiveness of flaps is different for controls starting at the wing root than for controls starting at the wing tip. Hence, in addition to the aforementioned restrictions placed on both methods, method I must be limited to the prediction of the lift characteristics of flaps starting at the wing tip only.

It was found in estimating the control parameters for the various wings that  $C_{L\delta}$  and  $C_{l\delta}$  could be estimated in about 1/2 to 1 hour by method I and  $C_{m\delta}$  (and incidentally  $C_{L\delta}$  and  $C_{l\delta}$ ) in about 3 to 4 hours by method II.

#### CONCLUDING REMARKS

An analysis has been made of the low-speed lift, rolling, and pitching characteristics of flap-type controls on a series of sweptback wings, and methods are presented for estimating these characteristics.

The methods of calculating the control effectiveness parameters give satisfactory results for sweptback wings having sweep angles from  $0^\circ$  to  $60^\circ$ , aspect ratios from 2.50 to 6.00, and taper ratios from 0.4

to 1.0. These methods are limited to the range wherein lift has a linear variation with both wing angle of attack and flap deflection.

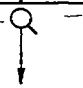

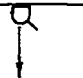


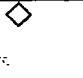
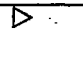
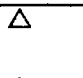
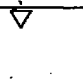
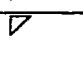
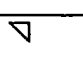
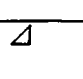
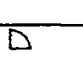
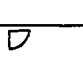
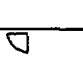
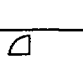
Langley Memorial Aeronautical Laboratory  
National Advisory Committee for Aeronautics  
Langley Field, Va., May 3, 1948

## REFERENCES

1. Pearson, Henry A., and Jones, Robert T.: Theoretical Stability and Control Characteristics of Wings with Various Amounts of Taper and Twist. NACA Rep. No. 635, 1938.
2. Weick, Fred E., and Jones, Robert T.: Résumé and Analysis of N.A.C.A. Lateral Control Research. NACA Rep. No. 605, 1937.
3. Langley Research Department: Summary of Lateral-Control Research. (Compiled by Thomas A. Toll.) NACA TN No. 1245, 1947.
4. Ames, Milton B., Jr., and Sears, Richard I.: Determination of Control-Surface Characteristics from NACA Plain-Flap and Tab Data. NACA Rep. No. 721, 1941.
5. Crane, Robert M.: Computation of Hinge-Moment Characteristics of Horizontal Tails from Section Data. NACA CB No. 5B05, 1945.
6. Swanson, Robert S., and Crandall, Stewart M.: Lifting-Surface-Theory Aspect-Ratio Corrections to the Lift and Hinge-Moment Parameters for Full-Span Elevators on Horizontal Tail Surfaces. NACA TN No. 1175, 1947.
7. Fischel, Jack, and Ivey, Margaret F.: Collection of Test Data for Lateral Control with Full-Span Flaps. NACA TN No. 1404, 1947.
8. Pitkin, Marvin, and Maggin, Bernard: Analysis of Factors Affecting Net Lift Increments Attainable with Trailing-Edge Split Flaps on Tailless Airplanes. NACA ARR No. 14118, 1944.
9. Street, William G., and Ames, Milton B., Jr.: Pressure-Distribution Investigation of an N.A.C.A. 0009 Airfoil with a 50-Percent-Chord Plain Flap and Three Tabs. NACA TN No. 734, 1939.
10. Ames, Milton B., Jr., and Sears, Richard I.: Pressure-Distribution Investigation of an N.A.C.A. 0009 Airfoil with a 30-Percent-Chord Plain Flap and Three Tabs. NACA TN No. 759, 1940.
11. Ames, Milton B., Jr., and Sears, Richard I.: Pressure-Distribution Investigation of an N.A.C.A. 0009 Airfoil with an 80-Percent-Chord Plain Flap and Three Tabs. NACA TN No. 761, 1940.
12. Swanson, Robert S., and Toll, Thomas A.: Jet-Boundary Corrections for Reflection Plane Models in Rectangular Wind Tunnels. NACA ARR No. 3E22, 1943.

TABLE I.—SUMMARY OF GEOMETRIC CHARACTERISTICS OF MODELS USED IN ANALYSIS

[Data obtained from wind-tunnel investigations at the Langley Laboratory<sup>a</sup>]

Model	Symbol notation for figures 12 to 16	$\Lambda$ (deg)	Type of test	Airfoil reference line	$\Lambda$	$\lambda$	$c_x^*/o^*$	Location of control		Air-flow characteristics	
								$\frac{y_1}{b/2}$	$\frac{y_0}{b/2}$	M	R
1		6.3	Semi-span	"Unswept" 0.50c	6.23	0.49	0.20	0.71 .42 .05	0.99 .99 .99	0.12	$1.55 \times 10^6$
2		30	Semi-span	"Unswept" 0.50c	5.26	.47	.184	.90 .67 .39 .05	.99 .99 .99 .99	.12	1.6
3		40	Semi-span	"Unswept" 0.50c	4.53	.46	.177	.87 .63 .35 .06	.99 .99 .99 .99	.12	1.8
4		51.3	Semi-span	"Unswept" 0.50c	3.43	.44	.167	.82 .59 .30 .06 .30 .06	.99 .99 .99 .99 .817 .585	.12	2.2
5		35	Semi-span	-----	6.0	.625	.272	.614	1.00	---	-----
6		45.1	Complete model	$\frac{c}{4}$	2.50	.425	.20	.50	1.00	.12	2.05
7		30	Complete wing	Wing L.E.	4.36	1.00	.20	.50	1.00	.17	1.15
8		45	Complete wing	Wing L.E.	3.56	1.00	.20	.50	1.00	.17	1.40
9		60	Complete wing	Wing L.E.	2.52	1.00	.20	.50	1.00	.17	1.98
10		45	Complete wing	Wing L.E.	2.61	1.00	.20	.50	1.00	.17	1.4
11		42.8	Complete model	$\frac{c}{4}$	4.00	.50	.20	.50	1.00	.16	2.15
12		38.7	Complete model	$\frac{c}{4}$	4.51	.54	.14	.515	1.00	.16	1.8
13		39	Complete model	-----	4.05	.54	.124	.515	1.00	.16	2.05
14		38	Complete model	$\frac{c}{4}$	3.01	.60	Tip 0.28c Root 0.22c	.47	.96	.4	2.8
15		42	Semi-span	$\frac{c}{4}$	4.01	.62	.20	.51	1.00	.11	2.30
16		42.8	Effectiveness of horizontal tail on complete model	-----	3.87	.49	.20	.04	1.00	.16	2.15

<sup>a</sup>Information for model 5 obtained from German investigation.

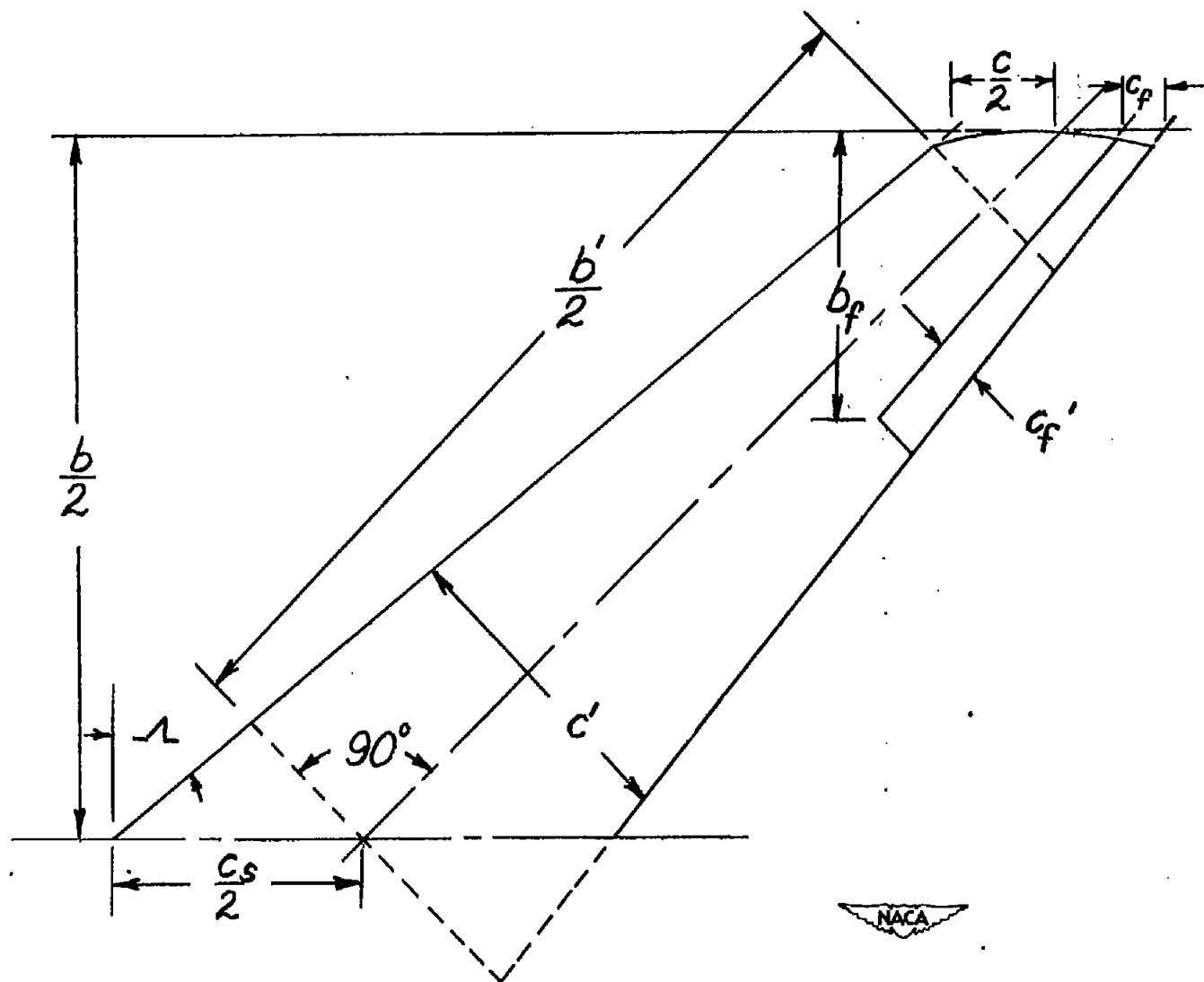


Figure 1.- Chords, spans, and sweep angle of swept and "unswept" wing.



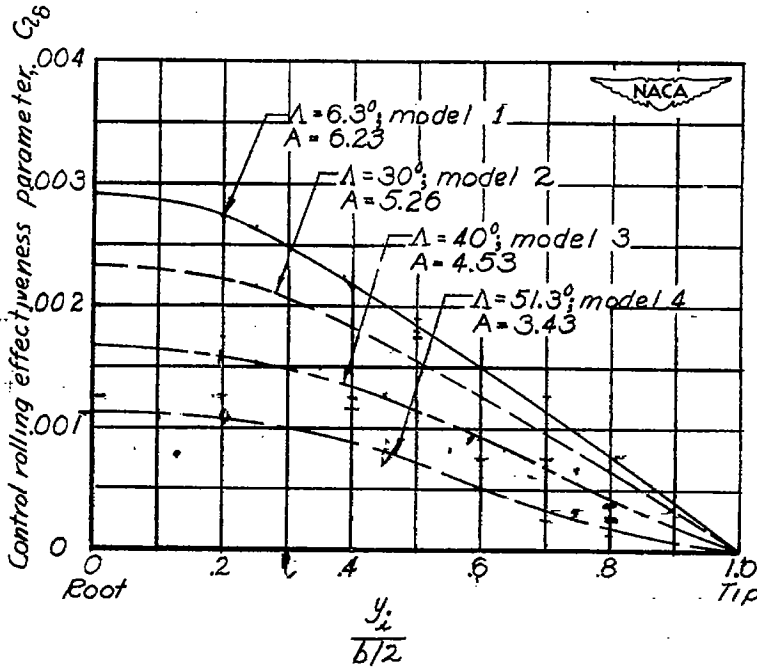


Figure 2.- Effect of sweep, aspect ratio, and span of control on rolling effectiveness parameter.  $\frac{y_0}{b/2} = 0.99$ .

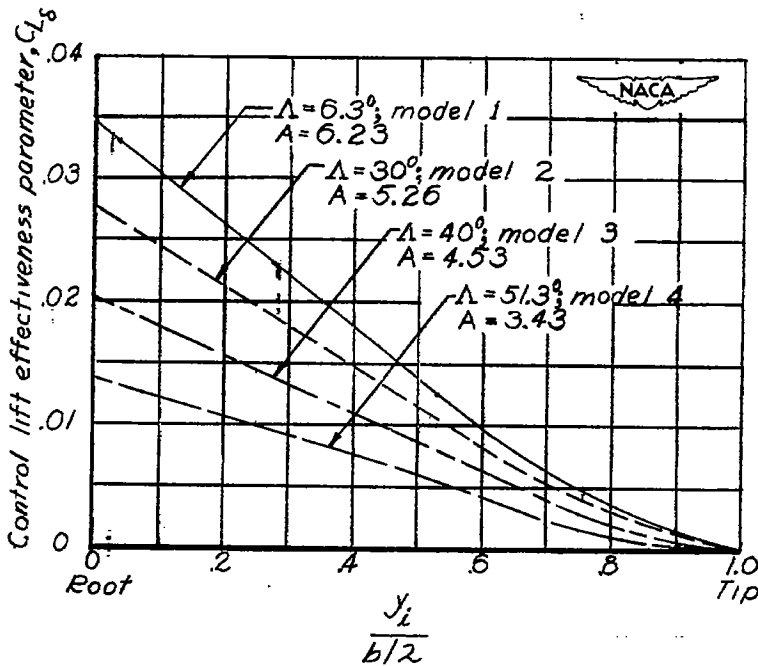


Figure 3.- Effect of sweep, aspect ratio, and span of control on lift effectiveness parameter.  $\frac{y_0}{b/2} = 0.99$ .

F-105  $C_{25}$  TN 1674 J. Lowry

$$C_{25} = \left( \frac{C_2}{\Delta \alpha} \right)_{u} K_1 K_2 \alpha_s \cos^2 \Delta$$

$$(C_2 / \Delta \alpha) = .0023$$

$$A' = 4.9 \quad c_f' / c' = .296 \quad \Delta \approx 47.9^\circ$$

$$\gamma' = .52$$

$$\cos 47.9^\circ = .670$$

$$\cos^2 47.9^\circ = .449$$

$$K_1 = .92 \quad K_2 = 1.01$$

$$\alpha_s = .575$$

$$C_{25} = .0023 \times .92 \times .575 \times .449$$

$$= .00055$$

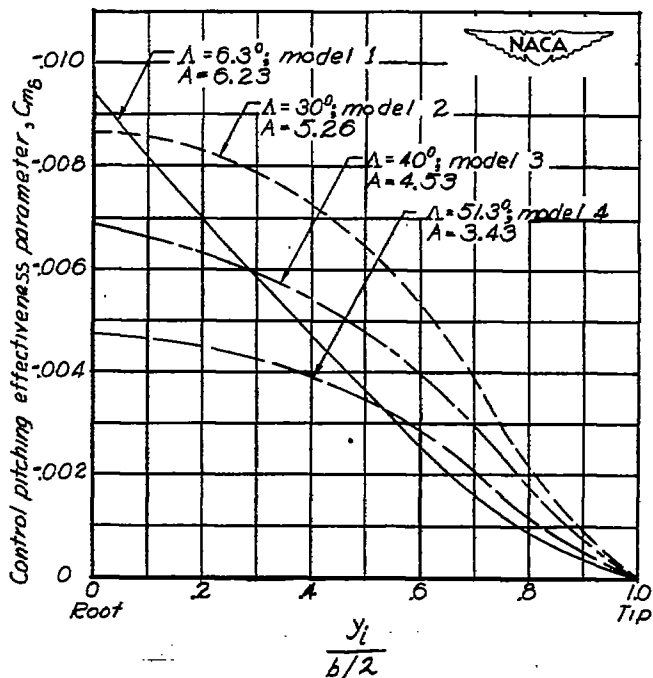


Figure 4.- Effect of sweep, aspect ratio, and span of control on pitching effectiveness parameter.  $\frac{y_0}{b/2} = 0.99$ .

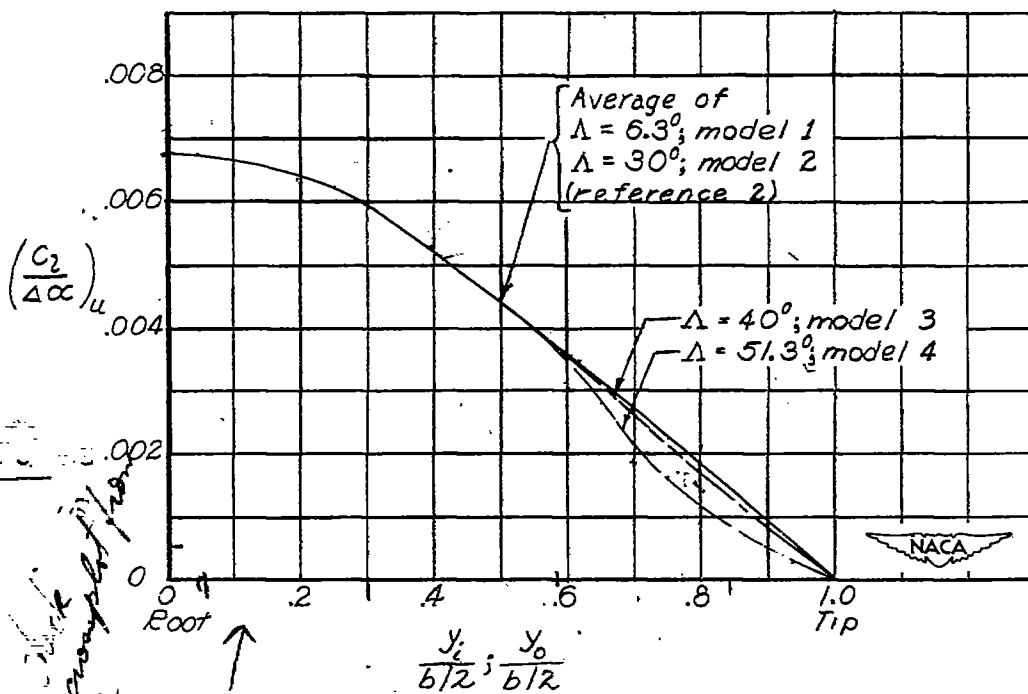


Figure 5.- Variation of theoretical and experimental values

of  $C_l / \Delta\alpha$  with flap span.  $C_{l\delta} = \left(\frac{C_l}{\Delta\alpha}\right)_u K_1 K_2 \alpha_\delta \cos^2 \Lambda$ .

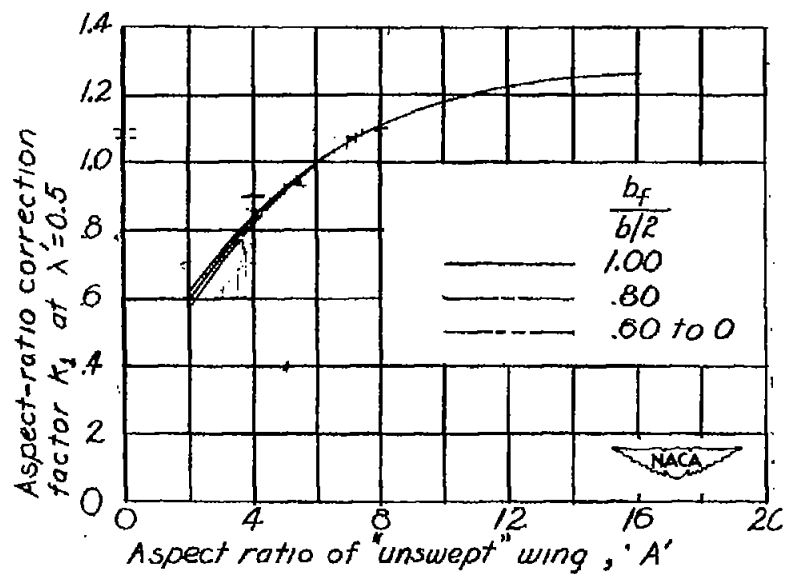
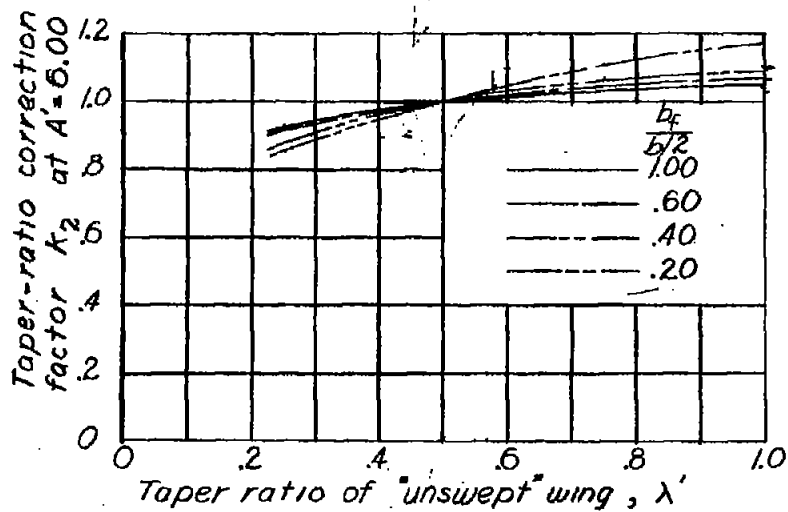


Figure 6.- Aspect-ratio and taper-ratio correction factors for calculating  $C_{L8}$ . (Curves calculated from data in reference 2.)

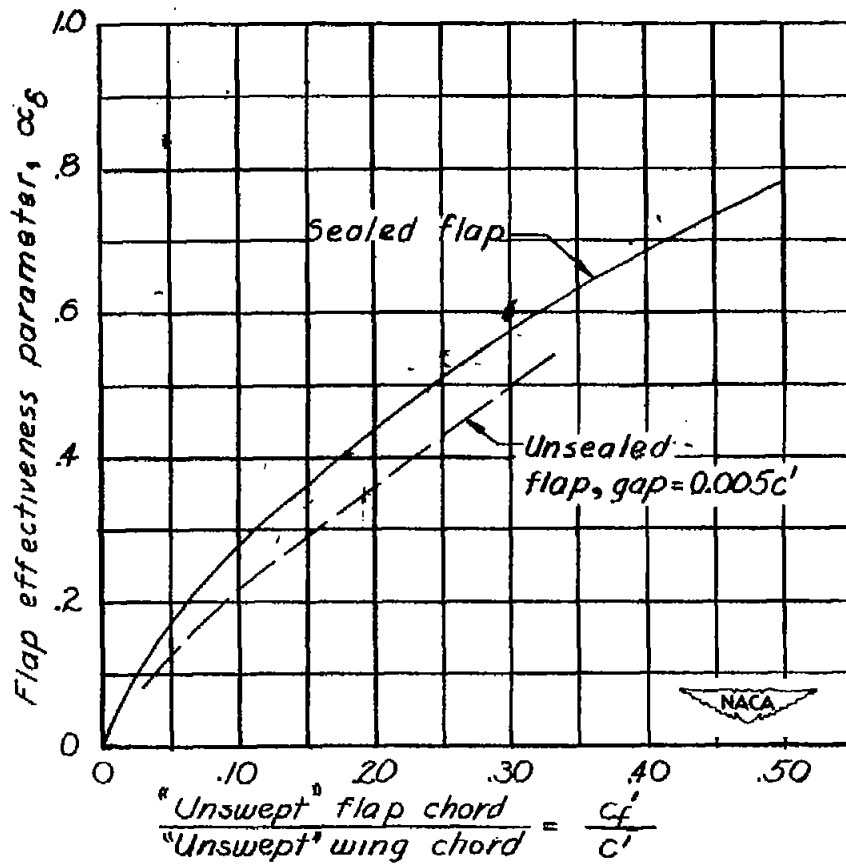


Figure 7.- Variation of flap effectiveness parameter with flap chord. (Data from reference 3.)

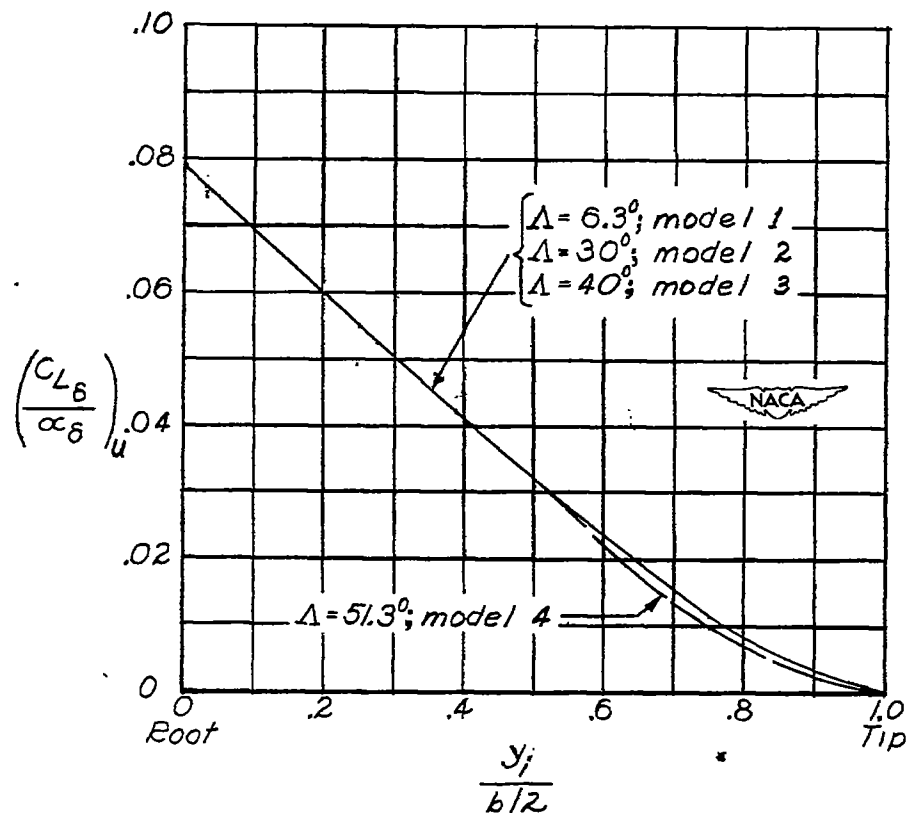


Figure 8.- Variation of experimental values of

$C_{L\delta}/\alpha_\delta$  with flap span.  $\frac{y_0}{b/2} = 1.00$ ;

$$C_{L\delta} = \left(\frac{C_{L\delta}}{\alpha_\delta}\right) \alpha_\delta K_3 \cos^2 \Delta.$$

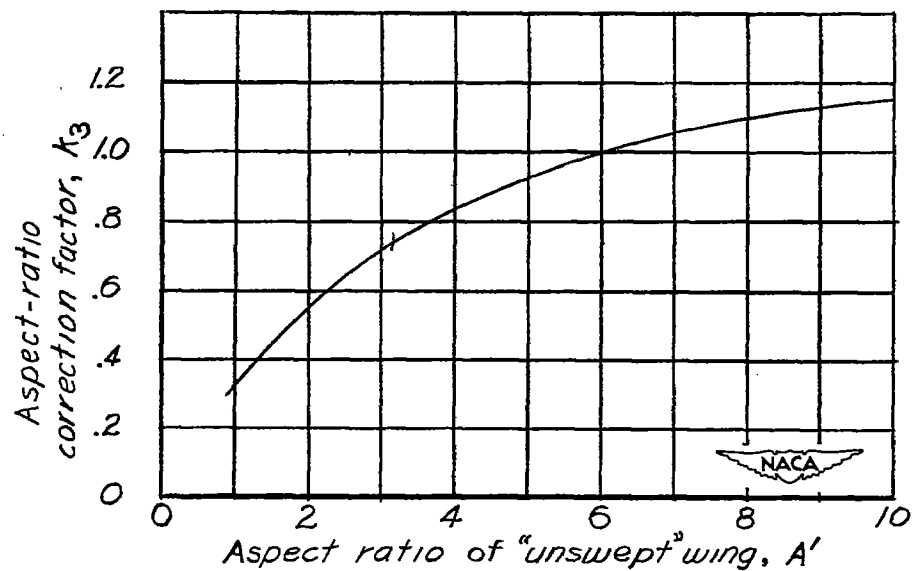


Figure 9.- Aspect-ratio correction factor for calculating  $C_{L\delta}$ . (Curve based on data obtained from the Langley 7- by 10-foot tunnel.)

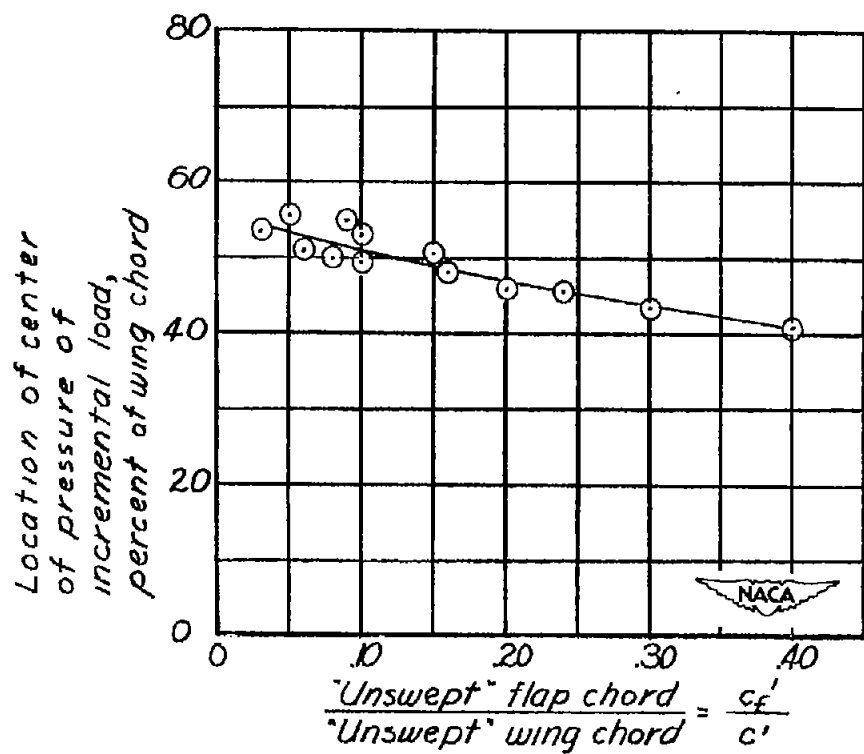


Figure 10.- Variation of center of pressure of incremental load with flap chord. (Data from references 8 to 11.)

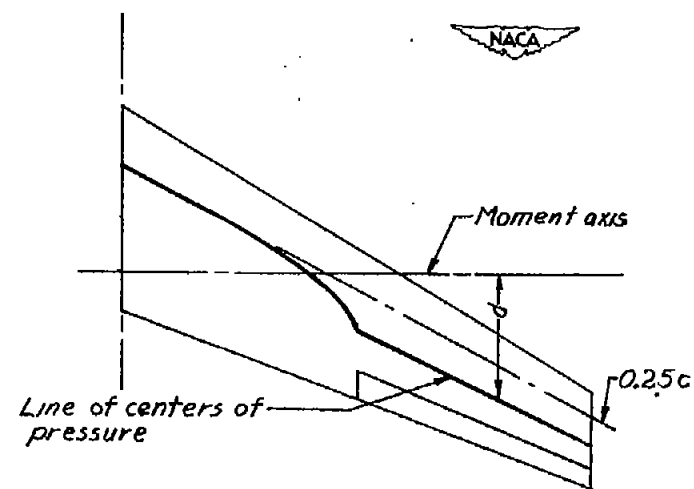
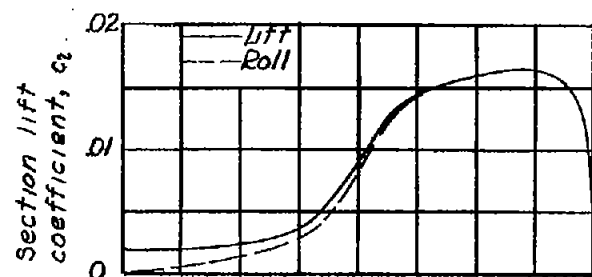
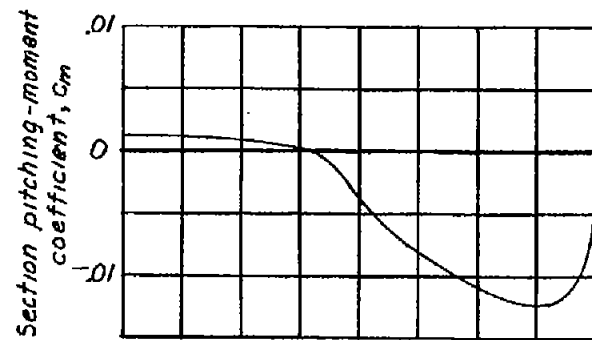


Figure 11.- Sample section lift and section pitching-moment coefficient distributions for a partial-span flap on a swept wing.

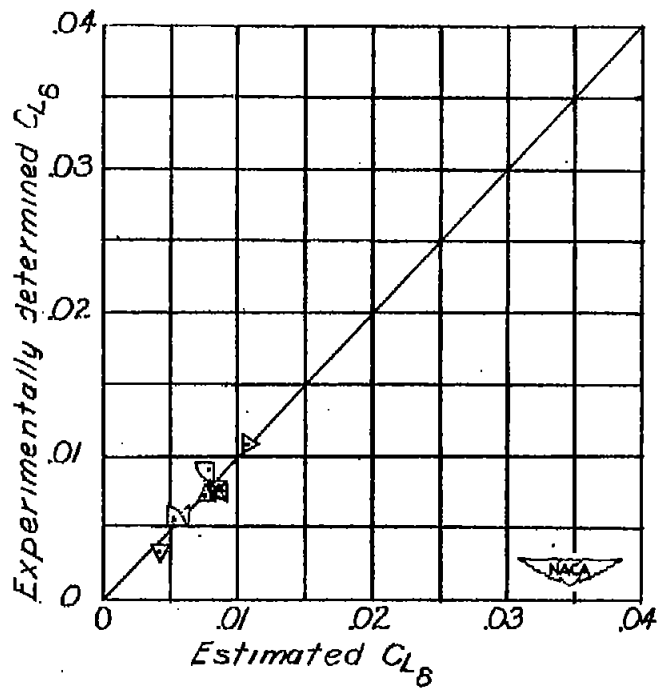


Figure 12.- Comparison of experimentally determined values of lift effectiveness parameter  $C_{L6}$  with values determined by method I. (Symbols refer to models listed in table I.)

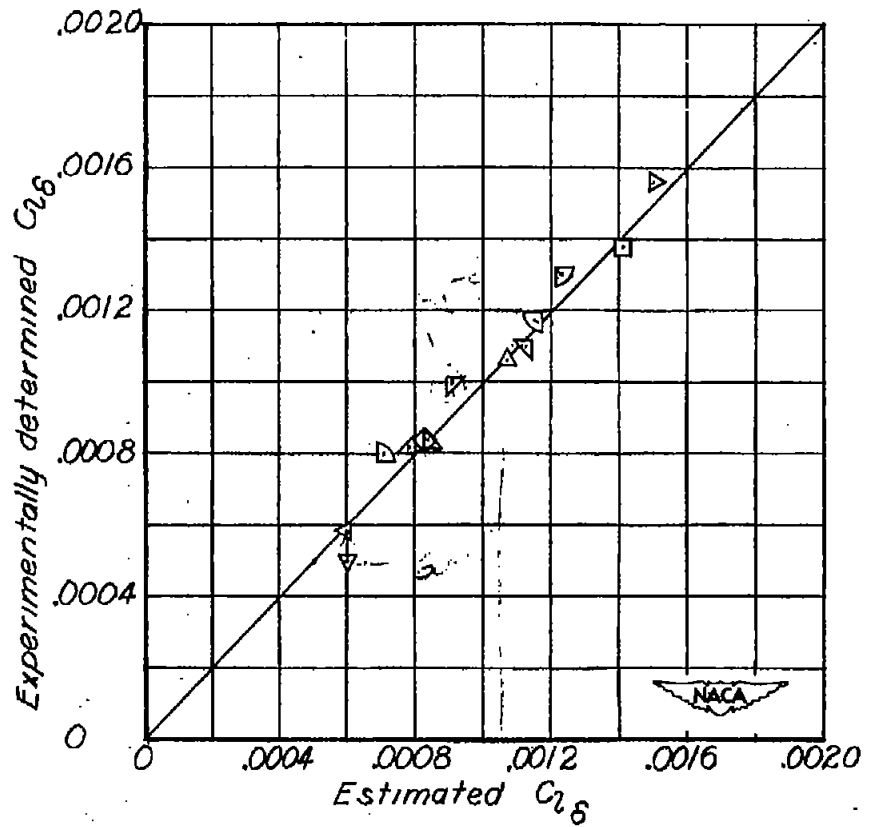


Figure 13.- Comparison of experimentally determined values of rolling effectiveness parameter  $C_{l6}$  with values determined by method I. (Symbols refer to models listed in table I.)

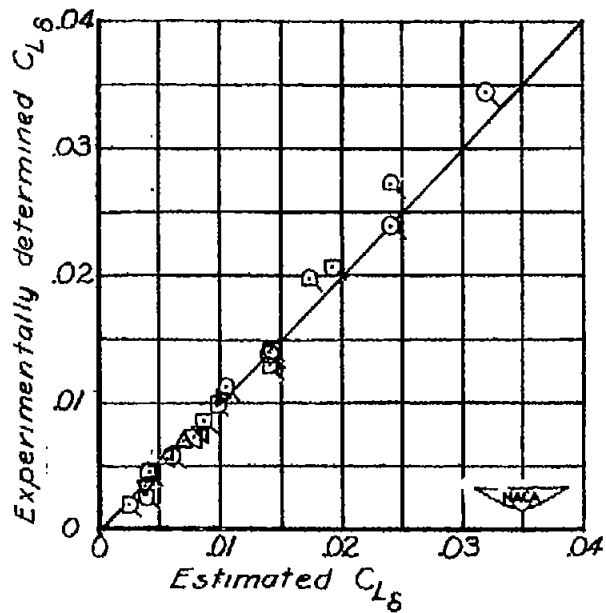


Figure 14.- Comparison of experimentally determined values of lift effectiveness parameter  $C_{L\delta}$

with values determined by method II. (Symbols refer to models listed in table I. Flagged symbols indicate comparison of estimated values with faired curves of fig. 3.)

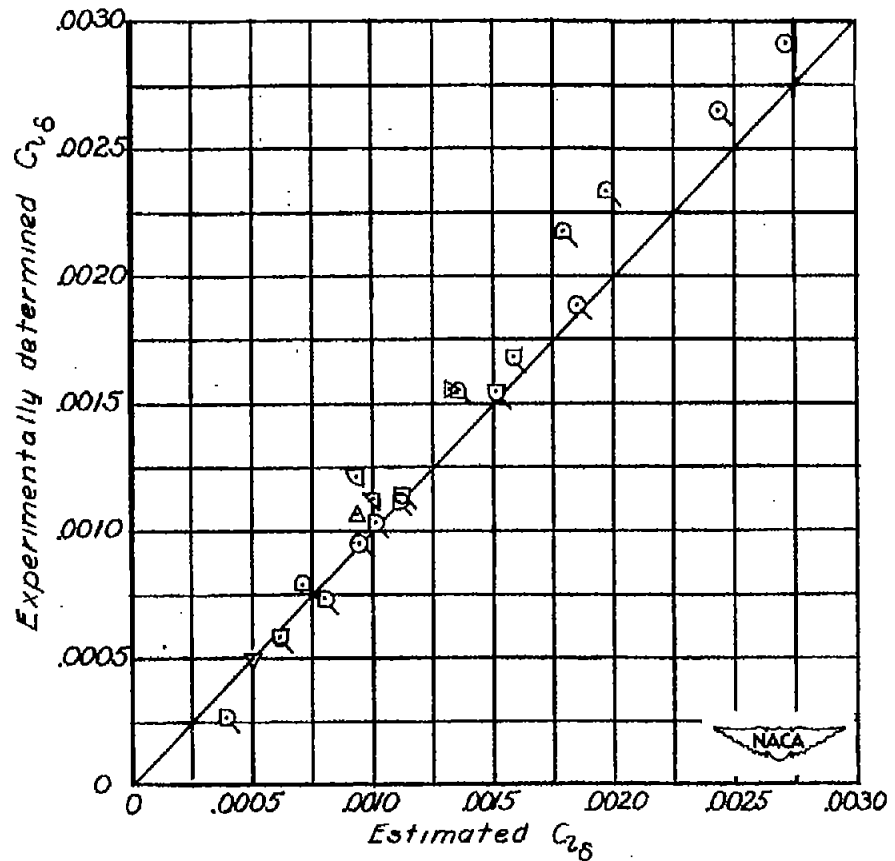


Figure 15.- Comparison of experimentally determined values of rolling effectiveness parameter  $C_{L\delta}$

with values determined by method II. (Symbols refer to models listed in table I. Flagged symbols indicate comparison of estimated values with faired curves of fig. 2.)



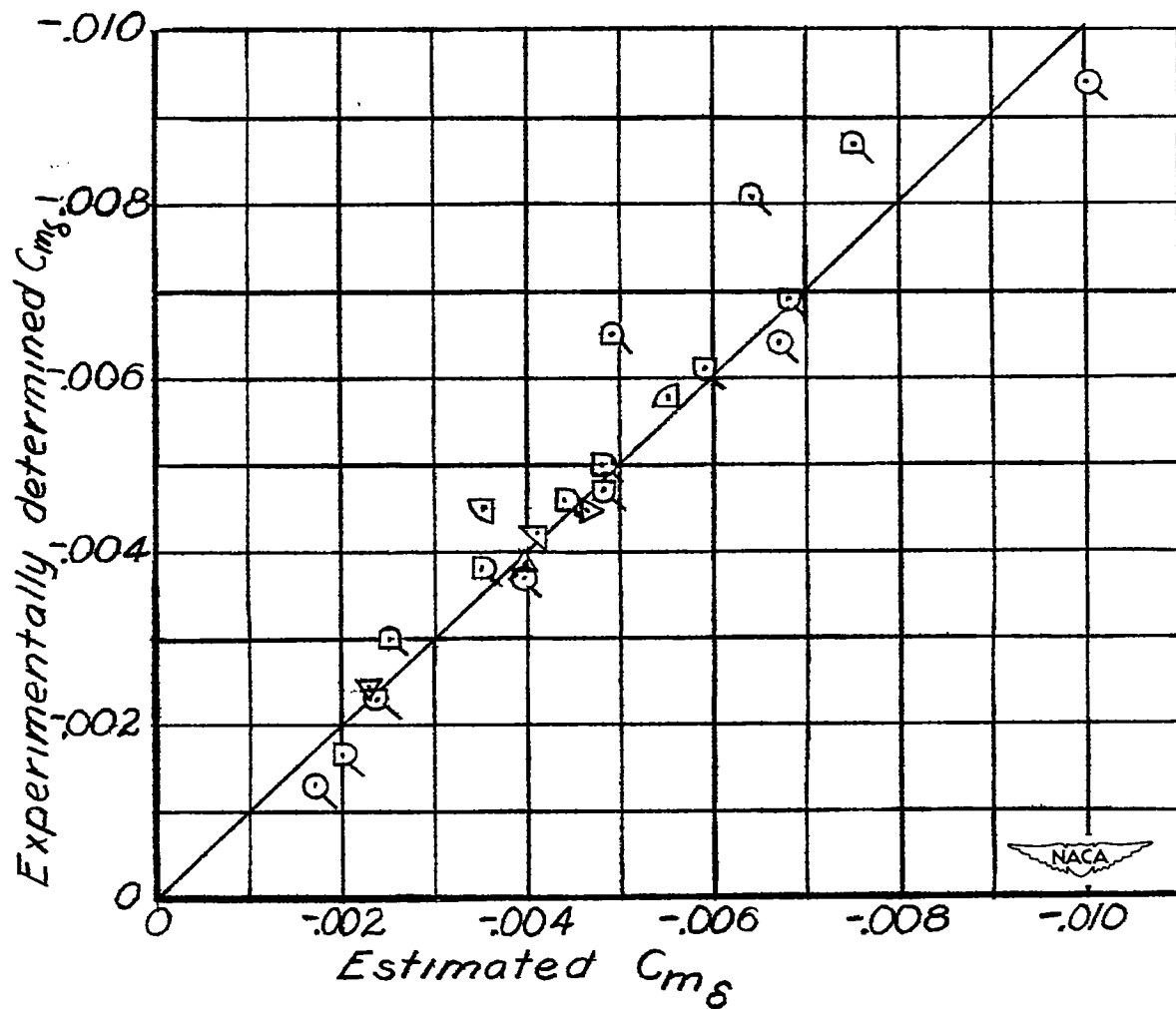


Figure 16.- Comparison of experimentally determined values of pitching effectiveness parameter  $C_{m\delta}$  with values determined by method II. (Symbols refer to models listed in table I. Flagged symbols indicate comparison of estimated values with faired curves of fig. 4.)